

# The inclusive reaction $d(\gamma, \pi)NN$ in the first resonance region

M.I. Levchuk<sup>a \*</sup>, M. Schumacher<sup>b †</sup> and F. Wissmann<sup>b ‡</sup>

<sup>a</sup> *B.I. Stepanov Institute of Physics, Belarus National Academy of Sciences,  
F. Scaryna prospect 70, 220072 Minsk, Belarus*

<sup>b</sup> *II Physikalisches Institut der Universität Göttingen,  
Bunsenstraße 7-9, D-37073 Göttingen, Germany*

## Abstract

Inclusive single pion photoproduction on the deuteron is studied in the first resonance region. The calculation is based on the use of the diagrammatic approach. Pole diagrams and one-loop diagrams with  $NN$  rescattering in the final state are taken into account. The elementary operator for pion photoproduction from the nucleon is taken in on-shell form and calculated using the SAID and MAID multipole analyses. Our predictions for total and differential cross section show good agreement with the available experimental data. Invoking some information on the reactions  $\gamma d \rightarrow \pi^0 d$  and  $\gamma d \rightarrow np$  we predict the total photoabsorption cross section for deuterium. We find that our results overestimate the experimental data in the center of the  $\Delta$ -peak ( $\sim 320$  MeV) by about 10%.

**PACS.** 13.60.Le meson production – 25.20.Lj photonuclear reactions

## I. INTRODUCTION

Recently, comprehensive measurements of total and differential cross sections of inclusive, coherent and incoherent  $\pi^0$ -photoproduction from the deuteron in the energy region from 200 to 792 MeV were carried out at MAMI [1]. It was found that the coherent data are in good agreement with theoretical predictions. However, in the case of the incoherent cross sections the situation is much less satisfactory. The theoretical predictions from Refs. [2,3] in the  $\Delta$ -region are significantly above the data. It is evident that the model of Ref. [3] can hardly provide a reasonable description of the data on pion photoproduction from the deuteron

---

\*E-mail: levchuk@dragon.bas-net.by

†E-mail: schumacher@physik2.uni-goettingen.de

‡E-mail: fwissma@gwdg.de

since it takes into account the pole diagrams only. It is known that the effect of nucleon-nucleon final state interaction (FSI) is extremely important in incoherent photoproduction especially for small pion angles (see Refs. [2,4,5]).

Although FSI was incorporated in the model of Ref. [2], it nevertheless failed to reproduce the data. A possible reason for this may be that Laget used in his calculations of the  $\gamma d \rightarrow \pi^0 np$  process the well-known Blomqvist-Laget (BL) parametrization [6] of the pion photoproduction amplitude on the nucleon. This parametrization gives a satisfactory fit to the amplitude for charged pion photoproduction. But it is not able to describe  $(\gamma, \pi^0)$  production from the proton. Since data on  $(\gamma, \pi^0)$  production from the neutron are absent there is no possibility to check the reliability of the BL model in the description of this channel. An attempt to remedy this defect in Ref. [7] led to a  $\pi^0$ -photoproduction amplitude which is not very suitable for the use in nuclear calculations.

In our previous analyses of  $\pi^0$ -photoproduction from the deuteron [4,5] we also used the BL operator. However, in those cases it was quite justified due to the following reasons. In Ref. [4] we studied the incoherent reaction  $d(\gamma, \pi^0 n)p$  in the  $\Delta$ -region in the neutron quasi-free kinematics. Our main purpose was to estimate the relative contributions of the neutron pole diagram and background effects due to FSI and  $\pi N$  rescattering. Since all these ingredients depend on the same pion photoproduction amplitude, the relative contributions are therefore not very sensitive to its magnitude. In Ref. [5] the reaction was considered in the threshold region. There, only the charged channels are of importance because of a big  $\pi^\pm N$  rescattering effect and the use of the BL operator is certainly possible.

In this article we present a new computation of the inclusive reaction  $d(\gamma, \pi^0)np$  in the first resonance region. The main difference between the present calculation and the one of Ref. [2] is, that a more realistic version of the elementary pion photoproduction operator is used. It is taken in the standard CGLN form [8] with four partial amplitudes  $F_i(\omega, \Theta_\pi)$  calculated with the use of the SAID [9] and MAID [10] multipole analyses <sup>1</sup>. Since a generalization of the approach into charged pion photoproduction is straightforward we take the opportunity to consider all possible inclusive channels  $d(\gamma, \pi)NN$  restricting ourselves, as in Ref. [4], to the first resonance region.

The paper is organized as follows. In Sect. II, kinematical relations used within calculations are briefly reviewed. A description of the theoretical model and its ingredients is given in Sect. III. In Sect. IV, we compare our results with all available experimental data. In Appendix A an extension of the non-relativistic approximations of the Bonn OBE potential is described, in order to make them applicable to  $nn$  and  $pp$  scattering. Kinematical relations between the variables in the so-called photon-nucleon c.m. frame and the ones in the  $\gamma d$  c.m. frame are given in Appendix B.

---

<sup>1</sup> An analogous method was used in Ref. [11] when considering the reaction  $d(\gamma, \gamma' n)p$ . Needed in practical calculations, the nucleon Compton scattering operator was taken in that work in on-shell form with partial amplitudes obtained in the framework of dispersion approach [12] (see also Ref. [13]).

## II. KINEMATICS

Let us denote by  $k = (k^0, \mathbf{k})$ ,  $p_d = (\varepsilon_d, \mathbf{p}_d)$ ,  $q = (\varepsilon_\pi, \mathbf{q})$ ,  $p_1 = (\varepsilon_1, \mathbf{p}_1)$  and  $p_2 = (\varepsilon_2, \mathbf{p}_2)$  the 4-momenta of the initial photon and deuteron, the final pion and nucleons, respectively. A symbol  $E_\gamma$  is reserved for the lab photon energy ( $k_{lab}^0 = E_\gamma$ ) and a symbol  $\omega$  will be used for the photon energy in the  $\gamma d$  c.m. frame:  $k_{cm}^0 = \omega = E_\gamma M / W_{\gamma d}$  with  $W_{\gamma d} = \sqrt{M^2 + 2ME_\gamma}$  and  $M$  being the deuteron mass.

It is convenient to take as independent kinematical variables the photon energy and pion momentum  $\mathbf{q}$  in the used frame of reference (generally, the lab or c.m. frame) and the angles  $\Theta_{\mathbf{P}}$  and  $\phi_{\mathbf{P}}$  of one of the nucleons in the c.m. frame of the final  $N_1 N_2$  pair. Using the equality

$$W_{NN} = 2\varepsilon_P = 2\sqrt{\mathbf{P}^2 + m^2} = \sqrt{(k + p_d - q)^2}, \quad (2.1)$$

where  $m$  is the averaged mass of the final nucleons, one can find the momentum  $\mathbf{P}$ . After boosting the momenta  $\mathbf{P}$  and  $-\mathbf{P}$  with the velocity  $(\mathbf{k} + \mathbf{p}_d - \mathbf{q}) / (k^0 + \varepsilon_d - \varepsilon_\pi)$  the momenta of the outgoing nucleons are obtained and, therefore, the kinematics is totally determined.

The differential cross section is given by

$$\frac{d\sigma}{d\mathbf{q}d\Omega_{\mathbf{P}}} = \frac{1}{(2\pi)^5} \frac{m^2 \varepsilon_d |\mathbf{P}|}{8k \cdot p_d \varepsilon_\pi \varepsilon_P} \frac{1}{6} \sum_{m_2 m_1 \lambda m_d} |\langle m_2 m_1 | T | \lambda m_d \rangle|^2, \quad (2.2)$$

where  $m_2$ ,  $m_1$ ,  $\lambda$ , and  $m_d$  are spin states of the two nucleons, photon, and deuteron, respectively. To obtain the inclusive differential cross section  $d\sigma/d\Omega_\pi$ , the r.h.s. of Eq. (2.2) has to be integrated over the value of the pion momentum  $q = |\mathbf{q}|$  and the solid angle  $\Omega_{\mathbf{P}}$ :

$$\frac{d\sigma}{d\Omega_\pi} = \int_0^{q^{max}} q^2 dq d\Omega_{\mathbf{P}} \frac{d\sigma}{d\mathbf{q}d\Omega_{\mathbf{P}}}. \quad (2.3)$$

An extra factor of 1/2 must be included in the r.h.s. of Eq. (2.3) in case of charged pion photoproduction. The maximum value  $q^{max}$  can be found from Eq. (2.1) at  $W_{NN} = 2m$ . In the c.m. frame it is given by

$$q^{max} = \frac{1}{2W_{\gamma d}} \sqrt{[W_{\gamma d}^2 - (2m + \mu)^2][W_{\gamma d}^2 - (2m - \mu)^2]}, \quad (2.4)$$

where  $\mu$  is the pion mass. In the lab frame one has

$$q^{max} = \frac{1}{b} \left[ a E_\gamma z + (E_\gamma + M) \sqrt{a^2 - b\mu^2} \right], \quad (2.5)$$

where  $a = (W_{\gamma d}^2 - 4m^2 + \mu^2)/2$  and  $b = (E_\gamma + M)^2 - E_\gamma^2 z^2$  with  $z = \cos \Theta_\pi$ .

## III. THE THEORETICAL MODEL FOR INCLUSIVE PION PHOTOPRODUCTION ON THE DEUTERON

As in our previous papers on  $\pi^0$ -photoproduction from the deuteron [4,5] we will exploit the diagrammatic approach to calculate the amplitude  $\langle m_2 m_1 | T | \lambda m_d \rangle$ . However, we reduce

the set of diagrams under consideration. For example, in Ref. [5] working in the threshold region we were forced to take into account a two loop diagram which includes simultaneously  $np$  and  $\pi N$  interactions. Such a diagram is of importance at threshold energies since it involves a block with charged pion photoproduction from the nucleon. With increasing photon energy this diagram becomes less important (see Ref. [5]). Above 200 MeV it can safely be disregarded. It is known (see Refs. [14,2]) that there are kinematical regions where a one loop diagram with  $\pi N$  rescattering noticeable contributes to the amplitude. But this rather concerns the exclusive process  $\gamma d \rightarrow \pi NN$ . We have checked that  $\pi N$  rescattering changes the final results in the first resonance region only by a few percent.

As a result, we retain in our calculations the two diagrams shown in Fig. 1. The pole diagram 1a must be considered since at the integrations in Eq. (2.3) there are the kinematical regions where one of nucleons (or both simultaneously) has a small momentum, the so-called quasi-free regions. These lead to peaks in the exclusive cross sections. The inclusive cross section from the pole diagrams is mainly saturated in these peaks. When at the integration mentioned above  $q$  is approaching  $q^{max}$  and, therefore,  $W_{NN} \rightarrow 2m$ , the relative momenta ( $\sim |\mathbf{P}|$ ) of the outgoing nucleons become small. Now there are peaks in the exclusive cross sections due to strong  $NN$  interaction in the  $s$ -waves (see, e.g., Refs. [14,2,11]) which manifest themselves in a big contribution of diagram 1b to the inclusive cross section. This effect is expected to be most pronounced at small pion angles since in this case the kinematics permits both for the deuteron wave function (DWF) and  $NN$  scattering amplitude to work simultaneously in low momentum regime. The above mentioned smallness of the  $\pi N$  rescattering effects can be explained also by the fact that the  $s$ -wave  $\pi N$  scattering lengths are about two orders smaller than those for  $NN$  scattering.

Let us now write out the matrix elements corresponding to the diagrams in Fig. 1 (see also Refs. [14,2,5]). One has for the pole diagram 1a

$$\langle m_2 m_1 | T^a(\mathbf{k}, \mathbf{q}, \mathbf{p}_2) | \lambda m_d \rangle = \sum_{\tilde{m}_1} \Psi_{m_2 \tilde{m}_1}^{m_d} \left( \mathbf{p}_2 - \frac{\mathbf{p}_d}{2} \right) \langle m_1 | T_{\gamma \tilde{N}_1 \rightarrow \pi N_1}(\mathbf{k}_{\pi N_1}, \mathbf{q}_{\pi N_1}) | \lambda \tilde{m}_1 \rangle, \quad (3.1)$$

where  $\Psi_{m_2 \tilde{m}_1}^{m_d}(\mathbf{p}_2 - \mathbf{p}_d/2)$  is DWF and  $\langle m_1 | T_{\gamma \tilde{N}_1 \rightarrow \pi N_1}(\mathbf{k}_{\pi N_1}, \mathbf{q}_{\pi N_1}) | \lambda \tilde{m}_1 \rangle$  is the amplitude of the elementary process  $\gamma N \rightarrow \pi N$ . The amplitude depends on photon ( $\mathbf{k}_{\pi N_1}$ ) and pion ( $\mathbf{q}_{\pi N_1}$ ) momenta taken in the c.m. frame of the  $\pi N_1$  pair. These momenta can be obtained from the corresponding momenta in the used frame of reference through a boost with the velocity  $(\mathbf{p}_2 - \mathbf{k} - \mathbf{p}_d)/(k^0 + \varepsilon_d - \varepsilon_2)$ .

Of course there is one more pole diagram identical to that in Fig. 1a but with the replacement  $1 \leftrightarrow 2$ . In case of  $\pi^0$ -photoproduction the corresponding matrix element should be added to Eq. (3.1). For the charged channels a subtraction of two matrix elements should be done.

The calculations were done using DWF for the non-relativistic versions of the Bonn OBE potential (OBEPR) [15,16]. In fact, in those papers three OBEPR models were built. A parametrization for one of them was given in Table 14 of Ref. [15]. Two other parametrizations were given in Table A.3 of Ref. [16] denoted in that table by ‘‘A’’ and ‘‘B’’. For these three versions we shall use the notations ‘‘OBEPR’’, ‘‘OBEPR(A)’’ and ‘‘OBEPR(B)’’, respectively. Analytical parametrizations of the  $s$ - and  $d$ -amplitudes of DWF for these three models were taken from Ref. [17]. We would like to note here that our results are practically independent of the choice of the potentials so that all results below were obtained with the OBEPR model.

It has been noted in Sect. I that in our previous papers [4,5] on  $\pi^0$ -photoproduction from the deuteron we used the BL operator to calculate the amplitude  $\langle m_1 | T_{\gamma \tilde{N}_1 \rightarrow \pi N_1} | \lambda \tilde{m}_1 \rangle$ . In the present paper the latter was obtained with the use of multipole analyses. The CGLN operator has the following form:

$$T_{\gamma N \rightarrow \pi N} = \frac{4\pi W_{\gamma N}}{m} [i\boldsymbol{\sigma} \cdot \boldsymbol{\epsilon}_\lambda F_1 + \mathbf{q} \cdot (\mathbf{k} \times \boldsymbol{\epsilon}_\lambda) F_2 + i\boldsymbol{\sigma} \cdot \mathbf{k} \mathbf{q} \cdot \boldsymbol{\epsilon}_\lambda F_3 + i\boldsymbol{\sigma} \cdot \mathbf{q} \mathbf{q} \cdot \boldsymbol{\epsilon}_\lambda F_4]. \quad (3.2)$$

It is written in the  $\pi N$  c.m. frame so that all vectors in Eq. (3.2) should be taken in this frame. Of course, the partial amplitudes  $F_i(\omega, \Theta_\pi)$  ( $i = 1 - 4$ ) are also functions of the photon energy  $\omega$  and pion angle  $\Theta_\pi$  in the same frame. Therefore, in practical calculations, in particular at the numerical integration in Eq. (2.3) (and in Eq. (3.3), see below) one has to make Lorentz transformations to this frame for every grid point. But such a procedure is of no principal difficulty and does not require time-consuming computations. We do not give here explicit expressions for the amplitudes  $F_i(\omega, \Theta_\pi)$  through electric and magnetic multipoles and the derivatives of the Legendre polynomials [8] since they are very well-known. The multipoles are taken from the SAID [9] and MAID [10] analyses. If not stated otherwise all results below have been obtained with the SAID multipoles.

The matrix element corresponding to diagram 1b is

$$\begin{aligned} & \langle m_2 m_1 | T^b(\mathbf{k}, \mathbf{q}, \mathbf{p}_2) | \lambda m_d \rangle = \\ & m \int \frac{d^3 \mathbf{p}_s}{(2\pi)^3} \sum_{\tilde{m}'_2 \tilde{m}'_1} \frac{\langle \mathbf{p}_{out}, m_2 m_1 | T_{NN} | \mathbf{p}_{in}, \tilde{m}'_2 \tilde{m}'_1 \rangle \langle \tilde{m}'_2 \tilde{m}'_1 | T^a(\mathbf{k}, \mathbf{q}, \mathbf{p}_s) | \lambda m_d \rangle}{p_{in}^2 - p_{out}^2 - i0}, \end{aligned} \quad (3.3)$$

where  $\mathbf{p}_{out} = (\mathbf{p}_2 - \mathbf{p}_1)/2$  and  $\mathbf{p}_{in} = \mathbf{p}_s + (\mathbf{q} - \mathbf{p}_d - \mathbf{k})/2$  are the relative momenta of the  $N_1 N_2$  pair after and before scattering, respectively, and  $\langle \mathbf{p}_{out}, m_2 m_1 | T_{NN} | \mathbf{p}_{in}, \tilde{m}'_2 \tilde{m}'_1 \rangle$  is the half off-shell  $NN$  scattering amplitude. We will not discuss here details of the computations of the amplitude (3.3) because they are given in Ref. [4]. Note that all partial waves with the total angular momentum  $J = 0$  and 1 were retained in the  $NN$  scattering amplitude. In fact, however, only two waves,  $^1S_0$  and  $^3S_1$ , are of importance when the inclusive channels are considered. All other waves give a few percent contribution to the cross section.

The same OBEPR models of  $NN$  interaction were used when solving the Lippmann-Schwinger equation for the  $NN$  scattering amplitude needed for the calculations of diagram 1b. It must be noted, however, that those models are valid for  $np$  interaction only. Therefore, they should be modified in such a way that they may be applicable to  $nn$  and  $pp$  interactions as well. We follow a procedure for such a modification proposed in Ref. [18]. It is described in some detail in Appendix A.

As in our previous papers [4,5], all summations over polarizations of the particles in Eqs. (3.1) and (3.3) as well as the three-dimensional integrations in Eq. (3.3) have been carried out numerically. The number of chosen nodes at this integration and that in Eq. (2.3) was taken to be sufficient for prediction of the differential cross section with the numerical accuracy better than 2%.

#### IV. RESULTS AND DISCUSSION

We begin our discussion with the results for the  $d(\gamma, \pi^0)np$  channel. In Fig. 2, the predicted differential cross sections of this reaction are shown at energies between 208 and 456

MeV together with experimental results from Ref. [1]<sup>2</sup>. One can see one more confirmation of a prediction of Refs. [2,4] that the effect of  $np$  final state interaction should lead to a reduction of the cross section and this reduction is the stronger the smaller the pion angles are. This effect is mainly attributed to the strong repulsive  $np$  interaction in the  ${}^3S_1$  wave.

Without FSI the model totally fails to reproduce the data. After including FSI one has a quite reasonable description of the data at all energies except for  $E_\gamma = 208$  MeV in the backward direction. Only the points corresponding to  $\Theta_\pi^{*N} = 110^\circ$  at energies from 285 to 362 MeV are noticeably below the curves. But it is difficult to draw smooth curves through the data if these points are included.

In the same figure we compare our results with those from Refs. [2,3]. Since in Ref. [3] FSI was disregarded one could expect the dotted curves to be close to the predictions of that work. In fact, one has some deviation which is reduced when the energy approaches the  $\Delta$ -position. A reason for this deviation may be due to the use of different pion photoproduction operators since the only remaining ingredient of the models, namely the deuteron wave functions, are very similar for all modern  $NN$  potentials. Indeed, a comparison of predictions for the total cross sections of the reaction  $\gamma p \rightarrow \pi^0 p$  given in Fig. 2 of Ref. [3] with those calculated with the SAID (and MAID) multipoles shows that these former go above the latter.

An analogous reason seems to be responsible for the disagreement between our full calculation and the predictions from Ref. [2] where FSI was taken into account. As already mentioned in Sect. I, the BL operator is not good for the description of neutral pion photoproduction. The deviation is clearly seen at  $\Theta_\pi^{*N} \geq 90^\circ$  above 300 MeV.

To illustrate, we show at 324 MeV the contribution from the pole diagram with  $\pi^0$ -photoproduction from the proton. A constructive effect of two mechanisms with quasi-free pion photoproduction on separate nucleons is obvious. One can see that at backward pion angles the total contribution of the pole diagrams is practically equal to the direct sum of the contributions of each diagram so that the interference term is very small. The reason for this is that at backward angles the kinematics does not allow both nucleons to have simultaneously small momenta and, therefore, both diagrams cannot work in the quasi-free regime.

After integrating Eq. (2.3) over the solid pion angle one obtains the total cross section for a given channel. In Fig. 3, the total cross section for  $\pi^0$ -photoproduction is shown. As in the case of the differential cross section, one can see that without FSI the model clearly overestimates the data. After inclusion of FSI one has good agreement with the data. Only in the center of the peak our model overestimates the measured cross sections by about 25  $\mu b$ . Note that the inclusion of FSI does not shift the position of this peak. This fact has a simple explanation. Indeed, diagram  $b$  in Fig. 1 contains the same  $\gamma N \rightarrow \pi N$  amplitude as the pole diagram  $1a$ . Taking into account that the integral over the loop is saturated at small momenta due to the deuteron wave function, the boosts mentioned in Sect. III lead only to small shifts in energies. Therefore, the  $\gamma N \rightarrow \pi N$  vertex works practically in the

---

<sup>2</sup> In Ref. [1] the differential cross sections are given in the so-called “photon-nucleon c.m. frame”. Relations needed to transform the cross sections and angles from the  $\gamma d$  c.m. frame to the frame mentioned are presented in Appendix B.

same energy regime as it does in the pole diagrams.

It is clear that the calculation of Ref. [3] totally fails to describe the data, as can be expected from the previous discussion. Although FSI was taken into account in Ref. [2], the predictions from that work give still too high cross sections.

We begin the discussion of charged pion photoproduction with the  $d(\gamma, \pi^-)pp$  channel. There is one experimental article [19] which supplies us with a lot of data points in the energy region from 0.2 to 2.0 GeV. However, we will discuss the first resonance region only. In Fig. 4 the predicted differential cross sections are shown at energies ranging from 210 to 540 MeV. The dotted curves which correspond to the contribution of one pole diagram, reproduce the behaviour of the angular dependence for the differential cross section of the elementary reaction  $\gamma n \rightarrow \pi^- p$ . In particular, at energies above 400 MeV the strong forward peak due to the contribution of the pion exchange in the  $t$ -channel is clearly seen. After inclusion of the second pole diagram one has a drastic reduction of the cross section at forward pion angles, exhibiting the total difference from the case of neutral pion photoproduction and showing how the Pauli principle manifests itself. One can again see that at backward angles the cross section from two pole diagrams is practically equal to twice the cross section from one diagram.

The effect of FSI in the case of the charged channels is expected to be quite different in comparison with the neutral one. Since only  $s$ -wave  $NN$  interaction is of importance for the inclusive  $d(\gamma, \pi)NN$  reaction, FSI shows up in the charged channels through attractive interaction in the  $^1S_0$  wave. This interaction is again significant at small pion angles but has to lead to an increase of the differential cross section. A confirmation of our anticipations is seen in Fig. 4. A very interesting observation is that above 400 MeV the cross section again becomes to be strongly forward peaked but now due to FSI. After inclusion of FSI we obtain good agreement with the data from Ref. [19].

At 350 MeV we compare our results with those from Ref. [2]. One can see that there is agreement in the shapes of the angular distributions but we predict lower values for the cross sections.

The total cross section for  $\pi^-$ -photoproduction is shown in Fig. 5. Here the contribution of FSI is noticeable smaller than that for  $\pi^0$ -production and leads to an increase of the cross section. We find good agreement with the data from Refs. [19] and [20] but the data from Ref. [21] lie above our solid curve at  $E_\gamma \geq 375$  MeV. At the same time a data pion from Ref. [22] at 250 MeV lies markedly below both our predictions and the data from Refs. [19] and [20]. Theoretical predictions from Refs. [2,3] are also shown in Fig. 5. They are very close to each other and are able to reproduce the data only below 250 MeV.

In Figs. 6 and 7 we give our results for  $\pi^+$ -photoproduction. All the theoretical conclusions we have just drawn for the case of  $\pi^-$ -photoproduction are valid for the  $\pi^+$  channel as well. To our knowledge there are no data on this process in the first resonance region so that we cannot compare our predictions with experimental results.

Having results for the total cross sections in all the channels mentioned above one can try to make predictions for the total photoabsorption cross section on the deuteron in the first resonance region. Of course, two more reactions contribute to it as well. These are coherent  $\pi^0$ -photoproduction from the deuteron ( $\gamma d \rightarrow \pi^0 d$ ) and deuteron photodisintegration ( $\gamma d \rightarrow np$ ). Predictions for the former are taken from a theoretical paper [23] which are in good agreement with the data from Ref. [1]. The total cross sections for the latter reaction were

calculated making use of a phenomenological fit [24] to available experimental data up to 440 MeV.

In Fig. 8 we present our results for the total photoabsorption cross section per nucleon for the deuteron. Good agreement with the data is seen excluding, however, the  $\Delta$ -peak region. In the center of the peak at about 320 MeV we find our results with SAID and MAID multipoles to overestimate the experimental value of  $(452 \pm 5) \mu b$  by  $33 \mu b$  and  $48 \mu b$ , respectively. We have no explanation for this disagreement.

It is instructive to compare the results of the direct measurements of the total photoabsorption cross section for the deuteron from Refs. [25,26] and those which can be extracted from the data on the separate channels contributing to this cross section. Let us try to put together all available data at 320 MeV. From Ref. [1] one has for the  $d(\gamma, \pi^0)np$  and  $d(\gamma, \pi^0)d$  channels  $(348 \pm 27) \mu b$  and  $(124 \pm 19) \mu b$ , respectively (the additional normalization error of 6% has been added). The result for the  $d(\gamma, \pi^-)pp$  channel from Refs. [19,20] is  $(249 \pm 10) \mu b$  (again the additional normalization error of 5% has been added). At 320 MeV the phenomenological fit [24] gives  $53 \mu b$  for the contribution of deuteron photodisintegration. The errors in this number can be safely neglected. Since there are no data on the  $d(\gamma, \pi^+)nn$  channel in the  $\Delta$ -region we accept for its contribution our theoretical prediction of  $199 \mu b$ . Collecting all these numbers we obtain the value of  $(487 \pm 17) \mu b$  for the total photoabsorption cross section per nucleon for the deuteron at 320 MeV which is in disagreement with the results from Refs. [25,26]. However, there exists good agreement with our values of  $485 \mu b$  and  $500 \mu b$  obtained with the SAID and MAID multipoles, respectively.

## V. SUMMARY

We have investigated inclusive single pion photoproduction on the deuteron in the first resonance region. Unlike most previous calculations, although not numerous, we have exploited as the elementary operator for pion photoproduction from the nucleon the one calculated with the SAID and MAID multipoles rather than the commonly used Blomqvist-Laget one or an operator built in Ref. [3]. We have found that the model involving the pole diagrams and FSI gives a good description of all available data both on the differential and total cross sections. This description is much better than that in other theoretical approaches. The only unsolved problem is that our predictions for the total photoabsorption cross section for the deuteron in the  $\Delta$ -peak region overestimate the data by about 10%. We suppose, however, that there is some inconsistency in the experimental results. New measurements, both inclusive single pion photoproduction on the deuteron in all inelastic channels and total photoabsorption cross section for the deuteron, would be extremely desirable and could shed more light on possible reasons for the above disagreement.

## ACKNOWLEDGMENTS

We would like to thank B. Krusche and A.I. L'vov for many fruitful discussions. We are very grateful to S.S. Kamalov for providing us with the results of his calculations and to R. Machleidt for a computer code for the CD-Bonn potential. This work was supported by Deutsche Forschungsgemeinschaft under contract 436 RUS 113/510.



## APPENDIX A: APPLICATION OF THE BONN OBEPR MODEL TO NEUTRON-NEUTRON AND PROTON-PROTON SCATTERING.

Used through this article the Bonn OBEPR model [15,16] is valid, strictly speaking, for  $np$  interaction only. Since in our consideration of charged pion photoproduction the amplitudes of  $nn$  and  $pp$  interactions are also needed we have to modify the potential so that it could be applicable to these interactions too. To do this we will use a procedure proposed in Ref. [18] which consists in adding Coulomb interaction to the original Bonn model and making small adjustments of the parameters of the model <sup>3</sup>.

A method to handle Coulomb interaction in momentum space was proposed by Vincent and Phatak [28]. We will not discuss it here since it is described in full detail in that article (see also Refs. [18,27,29]). We only mention that we applied the method to the  $^1S_0$  partial wave. All other waves with  $J = 0$  and 1 were taken for the switched off Coulomb potential. It makes no sense to include the Coulomb modifications for the waves other than  $^1S_0$ , since the contributions of these former to the differential and total cross sections were found to be very small.

Coulomb interaction is mainly responsible for the difference of the  $nn$  and  $pp$  scattering lengths. But the difference of the  $nn$  and  $np$  scattering lengths is due to the breaking of the charge independence of the nuclear force. The major reason for it is the pion mass splitting. This effect was not taken into account in the construction of the Bonn potentials. At least quantitatively, the differences above can be modelled by a procedure given in Ref. [18]. In that article it was proposed to vary the coupling constants of the  $\sigma NN$  (for the isospin  $I = 1$  channel) and  $\delta NN$  vertices keeping all other parameters of the model unchanged. These coupling constants were changed in such a way that the new model with the switched on Coulomb potential describes the  $^1S_0$  scattering length in the  $pp$  channel. At the same time in the  $^3S_1$ - $^3D_1$  partial wave there were the same deuteron properties as for the original version of the potential. Carrying out the proposed procedure we obtained the following coupling constants for the OBEPR, OBEPR(A) and OBEPR(B) models, respectively: 7.7135, 8.6226 and 8.7316 for  $g_\sigma^2/4\pi$  (*cf.* the former values 7.7823, 8.7171 and 8.8322) and 2.586, 2.81 and 6.744 for  $g_\delta^2/4\pi$  (*cf.* the former values 2.6713, 2.742 and 6.729). The resulting scattering lengths and effective ranges for three OBEPR models together with experimental values are given in Table I.

Solving the Lippmann-Schwinger equation with the original and modified versions of the OBEPR models we directly obtained the partial half-off shell amplitudes for  $np$  and  $nn$  scattering, respectively. For the  $pp$  scattering we used a prescription from Ref. [30] consisting of the following parametrization of the half-off-shell  $^1S_0$  partial amplitude:

$$t_{off}^{1S_0}(|\mathbf{p}_{out}|, |\mathbf{p}_{in}|) = \frac{|\mathbf{p}_{out}|^2 + \beta^2}{|\mathbf{p}_{in}|^2 + \beta^2} t_{on}^{1S_0}(|\mathbf{p}_{out}|, |\mathbf{p}_{out}|), \quad (\text{A1})$$

---

<sup>3</sup> It would be much more consistently to deal with a model which includes the charge dependence of nuclear forces and describes simultaneously all channels in  $NN$  interaction. Such a model called ‘CD-Bonn’ has recently been built by Machleidt [27]. Unfortunately, all our main calculations had already been finished when we got to know about the new potential. Very first estimates made with this potential show only small variations, within less than 1%, of the presented results.

with  $\beta = 1.2 \text{ fm}^{-1}$  and the on-shell amplitude  $t_{on}^{1S_0}(|\mathbf{p}_{out}|, |\mathbf{p}_{out}|)$  is obtained with the use of the Vincent and Phatak method for the modified potentials with switched on Coulomb interaction.

## APPENDIX B: KINEMATICAL RELATIONS BETWEEN THE VARIABLES IN PHOTON-NUCLEON C.M. FRAME AND THE $\gamma D$ C.M. FRAME.

In Ref. [1] the differential cross sections for the reaction  $d(\gamma, \pi^0)np$  are given in the so-called photon-nucleon c.m. frame. This latter corresponds to an assumption that all nucleons in a nucleus (we suppose the nucleus with mass number  $A$  but not only the deuteron) have the same momenta  $-\mathbf{k}/A$  in the  $\gamma A$  c.m. frame. This means that in the lab frame all nucleons in the nucleus are at rest and, therefore, the total energy of the  $\gamma N$  system is equal to  $W_{\gamma N} = \sqrt{m^2 + 2mE_\gamma}$ . The well known formulae give the photon energy and pion momentum in the  $\gamma N$  c.m. frame:

$$\omega^* = \frac{m}{W_{\gamma N}} E_\gamma, \quad q^* = \frac{1}{2W_{\gamma N}} \sqrt{[W_{\gamma N}^2 - (m + \mu)^2][W_{\gamma N}^2 - (m - \mu)^2]}, \quad (\text{B1})$$

and the pion energy is  $\varepsilon_\pi^* = \sqrt{q^{*2} + \mu^2}$ .

One can show that the photon energy and pion momentum in the frame where the nucleon has the momentum  $-\mathbf{k}/A$  are expressed through the following relations:

$$\tilde{\omega} = \frac{W_{\gamma N}^2 - m^2}{2\sqrt{\frac{W_{\gamma N}^2 + (A-1)m^2}{A}}}, \quad (\text{B2})$$

$$\tilde{q} = \frac{1}{b_1} \left[ a_1 \omega_A z + d \sqrt{a_1^2 - b_1 \mu^2} \right], \quad (\text{B3})$$

where  $a_1 = (d^2 - m^2 + \mu^2 - \omega_A^2)/2$ ,  $b_1 = d^2 - \omega_A^2 z^2$ ,  $d = \tilde{\omega} + \sqrt{(\tilde{\omega}/A)^2 + m^2}$ ,  $\omega_A = \tilde{\omega}(A-1)/A$  and  $z$  the cosine of the pion angle in the  $\gamma A$  c.m. frame. Of course, at  $A = 1$  one gets from Eqs. (B2) and (B3):  $\tilde{\omega} = \omega^*$  and  $\tilde{q} = q^*$ .

Using Eqs. (B1)–(B3) one can express  $z^{*N} = \cos \Theta_\pi^{*N}$  through  $z$

$$z^{*N} = \frac{\omega^* \varepsilon_\pi^* - (\tilde{\varepsilon}_\pi - \tilde{q}z)\tilde{\omega}}{\omega^* q^*}. \quad (\text{B4})$$

The derivative of  $z^{*N}$  with respect to  $z$  is then given by

$$\frac{\partial z^{*N}}{\partial z} = \frac{\tilde{\omega}}{\omega^* q^*} \left[ \left( z - \frac{\tilde{q}}{\tilde{\varepsilon}_\pi} \right) \frac{\partial \tilde{q}}{\partial z} + \tilde{q} \right]. \quad (\text{B5})$$

Presented in Fig. 2 the differential cross sections and angles  $\Theta_\pi^{*N}$  were obtained making use of Eqs. (B4)–(B5) for  $A = 2$ .

## REFERENCES

- [1] B. Krusche et al., *Eur. Phys. J. A* **6**, 309 (1999).
- [2] J.M. Laget, *Phys. Rep.* **69**, 1 (1981).
- [3] R. Schmidt, H. Arenhövel and P. Wilhelm, *Z. Phys. A* **355**, 421 (1996).
- [4] M.I. Levchuk, V.A. Petrun'kin and M. Schumacher, *Z. Phys. A* **355**, 317 (1996).
- [5] M.I. Levchuk, M. Schumacher and F. Wissmann, *Nucl. Phys. A* **675**, 621 (2000).
- [6] I. Blomqvist and J.M. Laget, *Nucl. Phys. A* **280**, 405 (1977).
- [7] J.L. Sabutis, *Phys. Rev. C* **27**, 778 (1983).
- [8] G.F. Chew, M.L. Goldberger, F.E. Low and Y. Nambu, *Phys. Rev.* **106**, 1345 (1957).
- [9] R.A. Arndt, I.I. Strakovsky and R.L. Workman, *Phys. Rev. C* **53**, 430 (1996); *Phys. Rev. C* **56**, 577 (1997), and the code SAID, solution SM00K.
- [10] D. Drechsel, O. Hanstein, S.S. Kamalov and L. Tiator, *Nucl. Phys. A* **645**, 145 (1999), and the code MAID 2000.
- [11] M.I. Levchuk, A.I. L'vov and V.A. Petrun'kin, *Few-Body Systems* **16**, 101 (1994).
- [12] A.I. L'vov, V.A. Petrun'kin and S.A. Startsev, *Yad. Fiz.* **29**, 1265 (1979) [*Sov. J. Nucl. Phys.* **29**, 651 (1979)].
- [13] A.I. L'vov, V.A. Petrun'kin and M. Schumacher, *Phys. Rev. C* **55**, 359 (1997).
- [14] J.M. Laget, *Nucl. Phys. A* **296**, 388 (1978).
- [15] R. Machleidt, K. Holinde and Ch. Elster, *Phys. Rep.* **149**, 1 (1987).
- [16] R. Machleidt, *Adv. Nucl. Phys.* **19**, 189 (1989).
- [17] M.I. Levchuk, *Few-Body Systems* **19**, 77 (1995).
- [18] J. Haidenbauer and K. Holinde, *Phys. Rev. C* **40**, 2465 (1989).
- [19] P. Benz et al., *Nucl. Phys. B* **65**, 158 (1973).
- [20] G. Chiefari, E. Drago, M. Napolitano and C. Sciacca, *Lett. Nuovo Cim.* **13**, 129 (1975).
- [21] M. Asai et al., *Phys. Rev. C* **42**, 837 (1990).
- [22] M.A. Quraan et al., *Phys. Rev. C* **57**, 2118 (1998).
- [23] S.S. Kamalov, L. Tiator and C. Bennhold, *Phys. Rev. C* **55**, 98 (1997) and S.S. Kamalov, private communication.
- [24] P. Rossi et al., *Phys. Rev. C* **40**, 1412 (1989).
- [25] T.A. Armstrong et al., *Nucl. Phys. B* **41**, 445 (1972).
- [26] M. MacCormick et al., *Phys. Rev. C* **53**, 41 (1996).
- [27] R. Machleidt, *nucl-th/0006014*.
- [28] C.M. Vincent and S.C. Phatak, *Phys. Rev. C* **10**, 391 (1974).
- [29] B. Holzenkamp, K. Holinde and J. Speth, *Nucl. Phys. A* **500**, 485 (1989).
- [30] V.M. Kolybasov and V.G. Ksenzov, *Yad. Fiz.* **22**, 720 (1975) [*Sov. J. Nucl. Phys.* **22**, 372 (1976)].
- [31] C.R. Howell et al., *Phys. Lett. B* **444**, 252 (1998).
- [32] D.E. González Trotter et al., *Phys. Rev. Lett.* **83**, 3788 (1999).
- [33] G.A. Miller, M.K. Nefkens and A. Slaus, *Phys. Rep.* **194**, 1 (1990).
- [34] J.R. Bergervoet, P.C. van Campen, W.A. van der Sanden and J.J. de Swart, *Phys. Rev. C* **38**, 15 (1988).

TABLE I. Effective range parameters of the  $^1S_0$  wave.

	<i>nn</i> channel		<i>pp</i> channel	
	$a_s$ (fm)	$r_s$ (fm)	$a_s$ (fm)	$r_s$ (fm)
OBEPR	-17.78	2.71	-7.82	2.64
OBEPR(A)	-17.82	2.75	-7.82	2.62
OBEPR(B)	-17.73	2.76	-7.82	2.63
Experiment	$-18.9 \pm 0.4$ [31,32]	$2.75 \pm 0.11$ [33]	$-7.8149 \pm 0.0026$ [34]	$2.790 \pm 0.014$ [34]

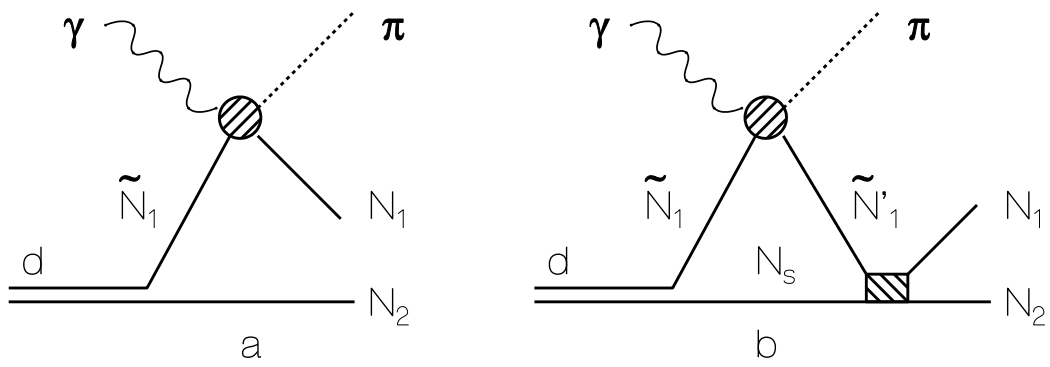


FIG. 1. Diagrams considered in this work. Two other diagrams with the permutation  $1 \leftrightarrow 2$  are assumed.

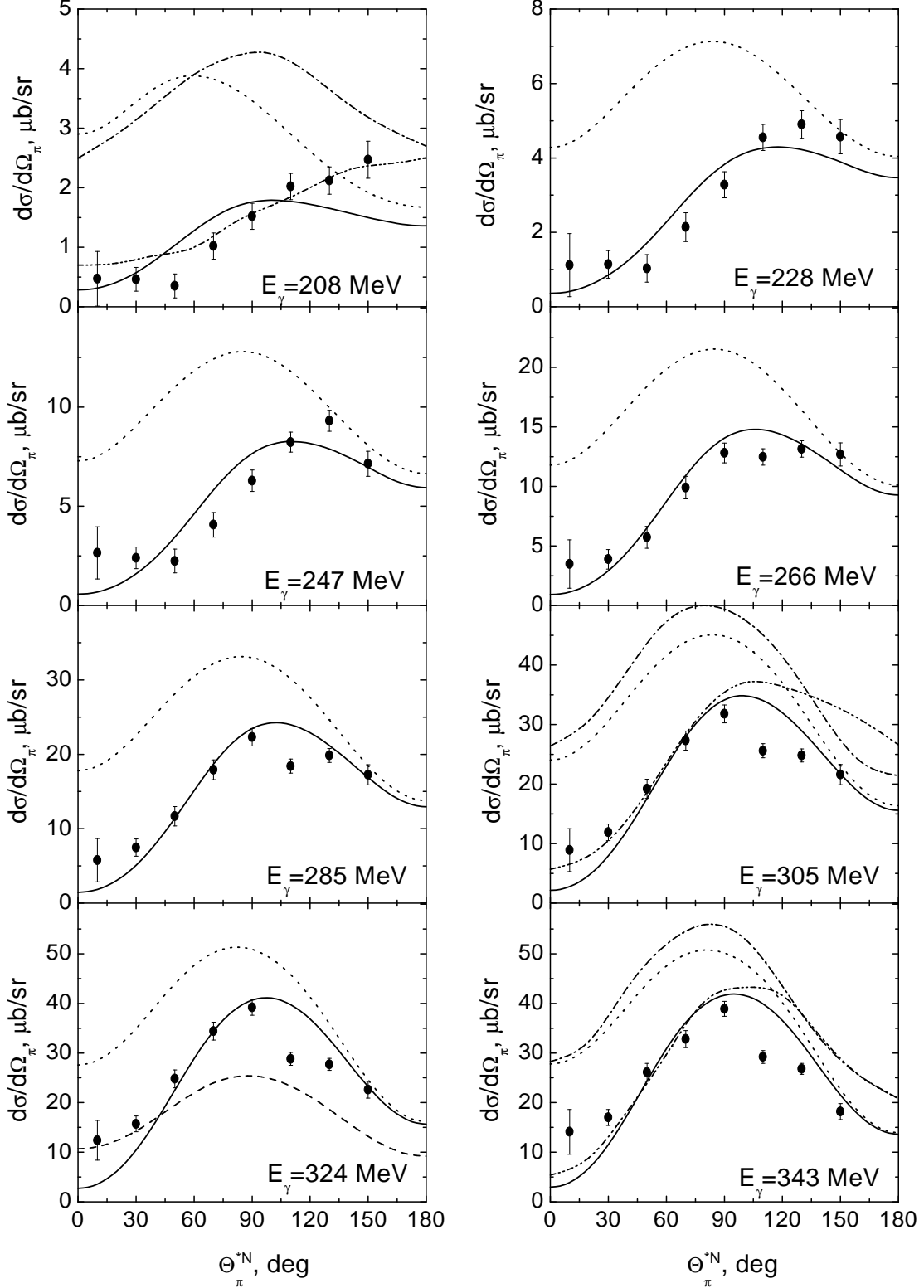


FIG. 2. Differential cross sections for the reaction  $d(\gamma, \pi^0)np$  in the photon-nucleon c.m. frame. The dotted (full) curves are our predictions without (with) FSI. At 324 MeV the contribution of the pole diagram with pion production from the proton is shown in dashed curve. The dash-double-dotted and dash-dotted curves are results of Refs. [2] and [3], respectively, borrowed from Ref. [1]. Data are from Ref. [1].

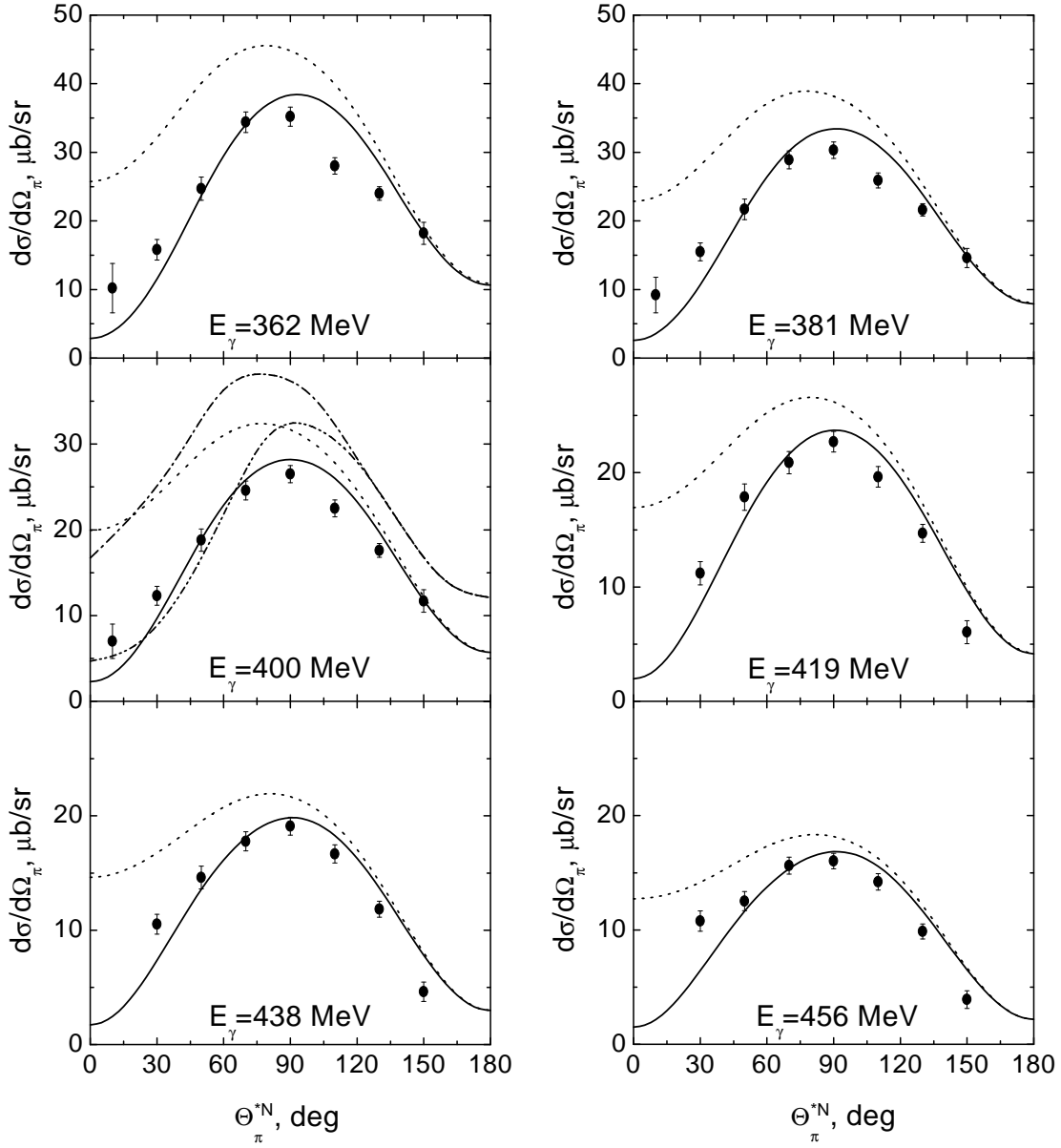


FIG. 2. Continued.

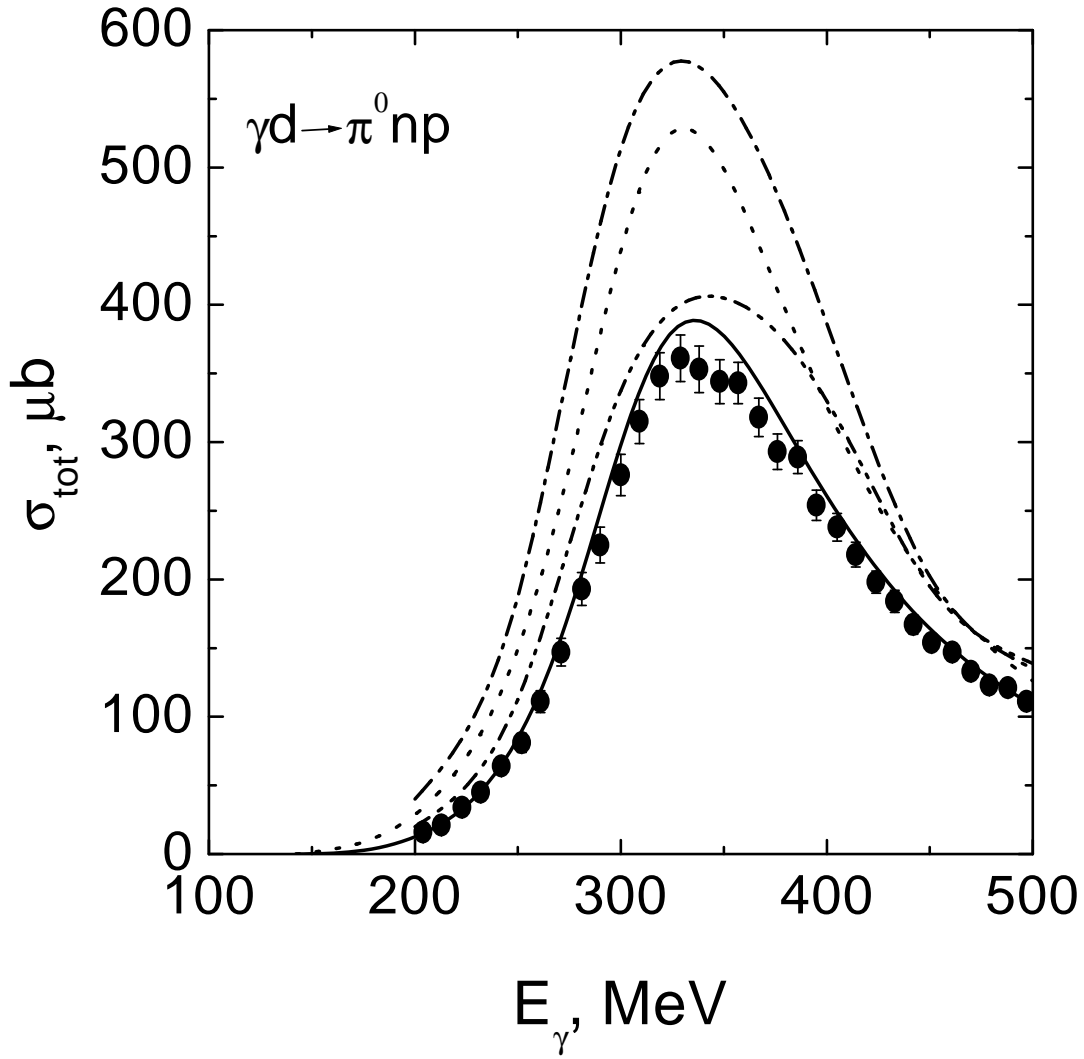


FIG. 3. Total cross section for the reaction  $d(\gamma, \pi^0)np$ . Meaning of the curves as in Fig. 2. Data are from Ref. [1].



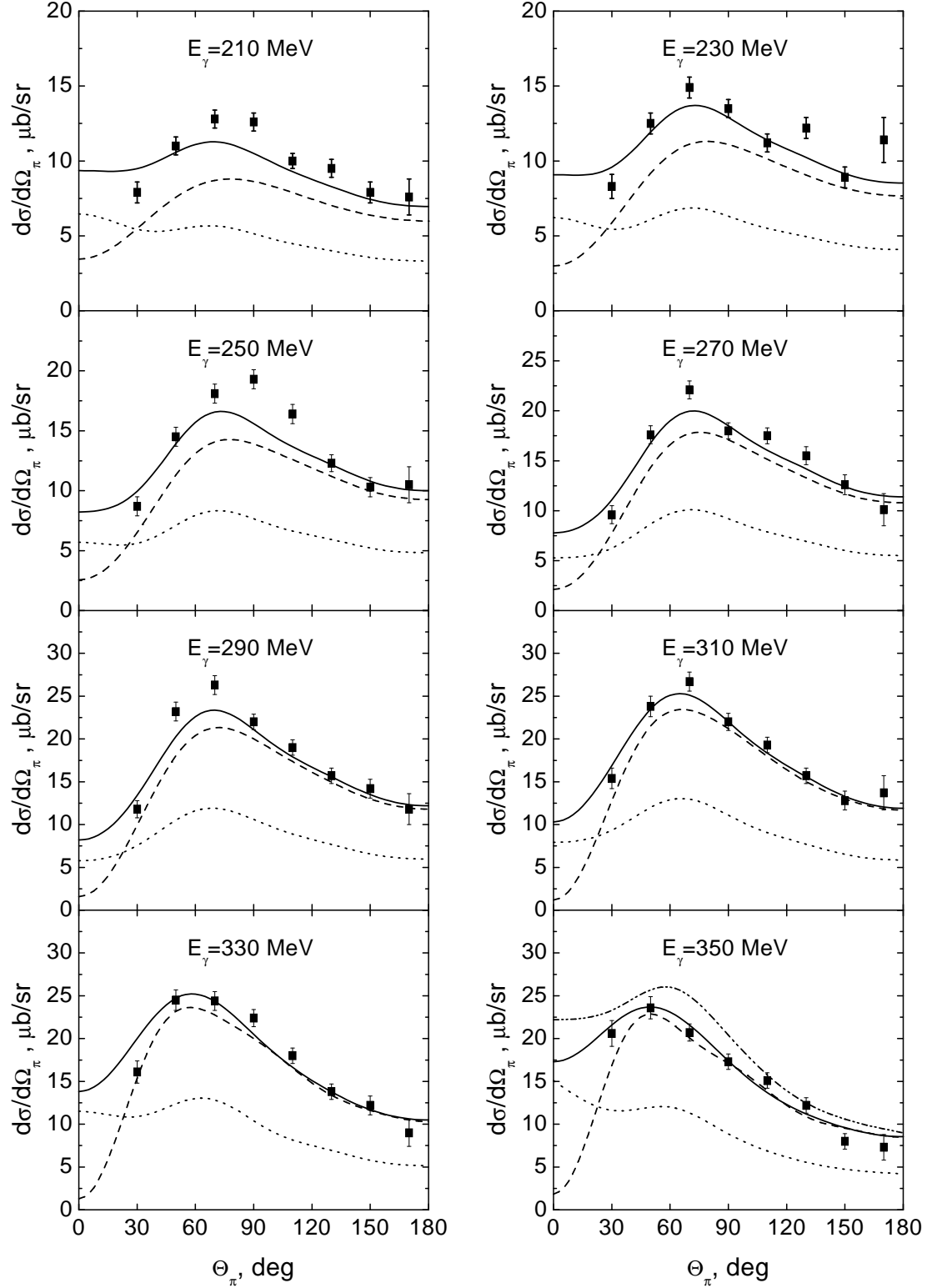


FIG. 4. Differential cross sections for the reaction  $d(\gamma, \pi^-)pp$  in the lab frame. The dotted curves are contributions of one of the pole diagrams in Fig. 1. Successive addition of the second pole diagram and FSI leads to dashed and full curves, respectively. At 350 MeV the results from Ref. [2] are shown as a dash-double-dotted curve. Data are from Ref. [19].

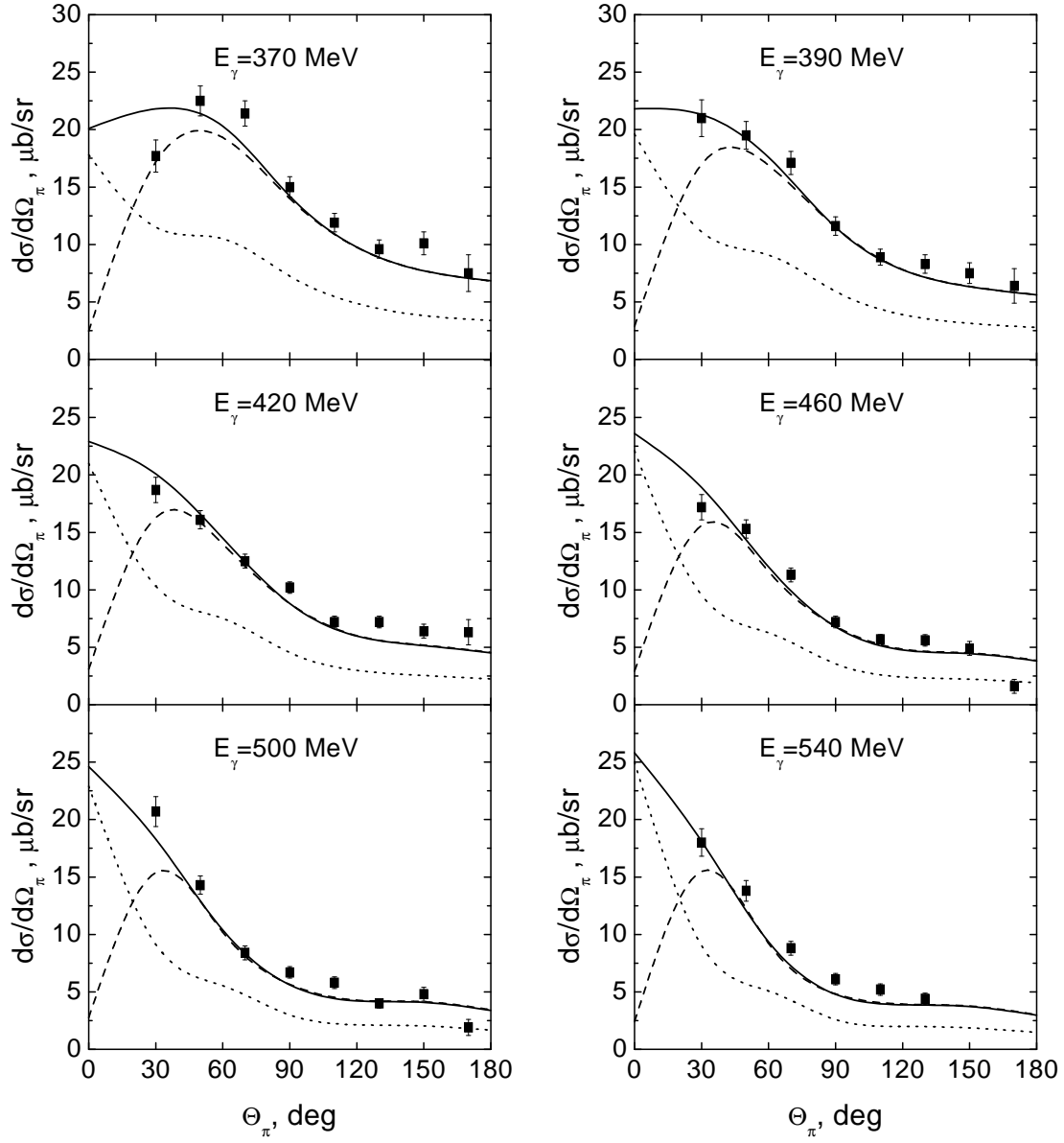


FIG. 4. Continued.

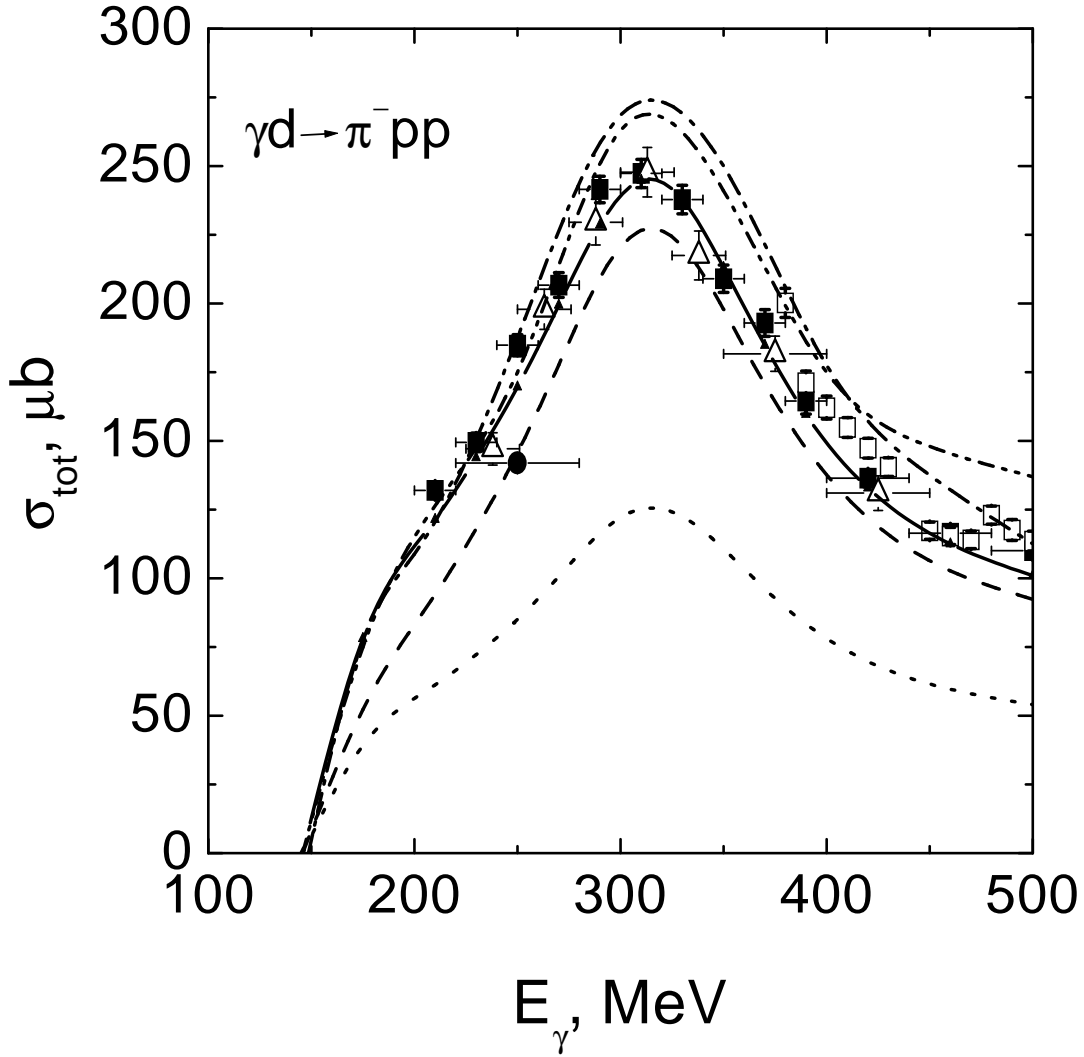


FIG. 5. Total cross section for the reaction  $d(\gamma, \pi^-)pp$ . Meaning of the curves as in Fig. 4. In addition the results from Refs. [2] and [3] are shown in dash-double-dotted and dash-dotted curves, respectively. Data are from Refs. [19] (solid boxes), [20] (empty triangles), [21] (empty boxes), and [22] (solid circle).

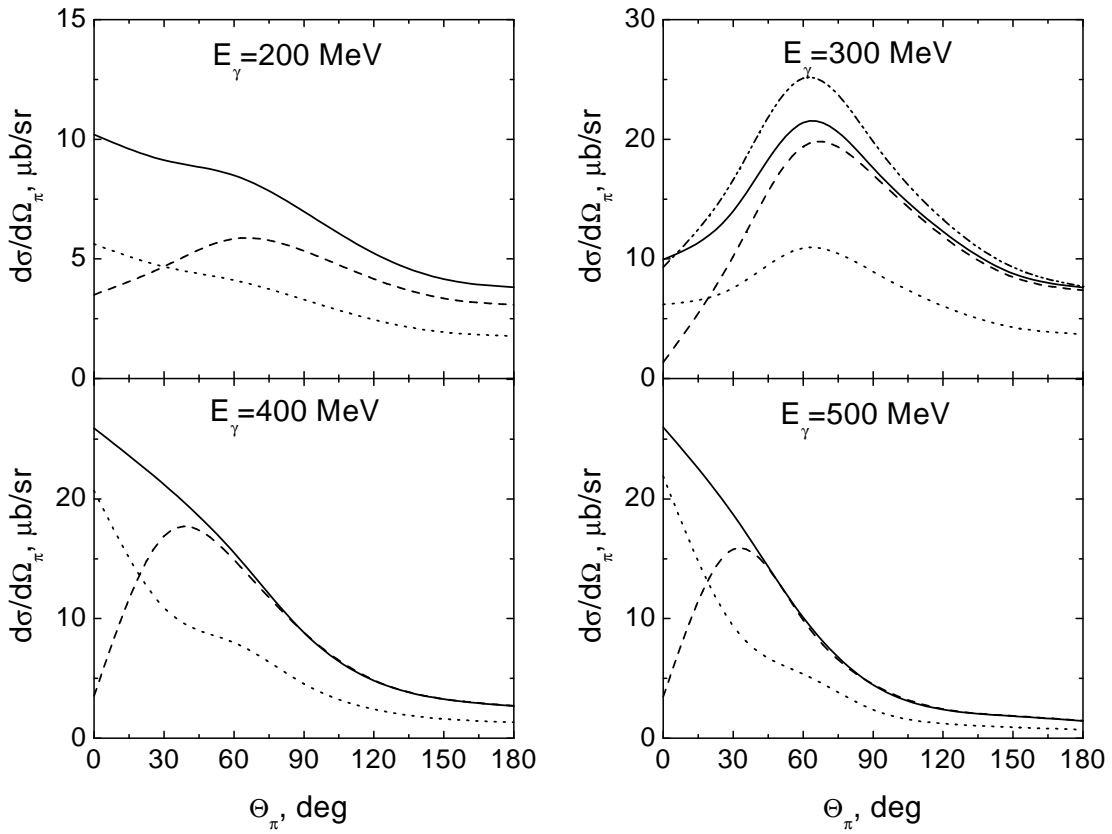


FIG. 6. Differential cross sections for the reaction  $d(\gamma, \pi^+)nn$  in the lab frame at four energies. Meaning of the curves as in Fig. 4.

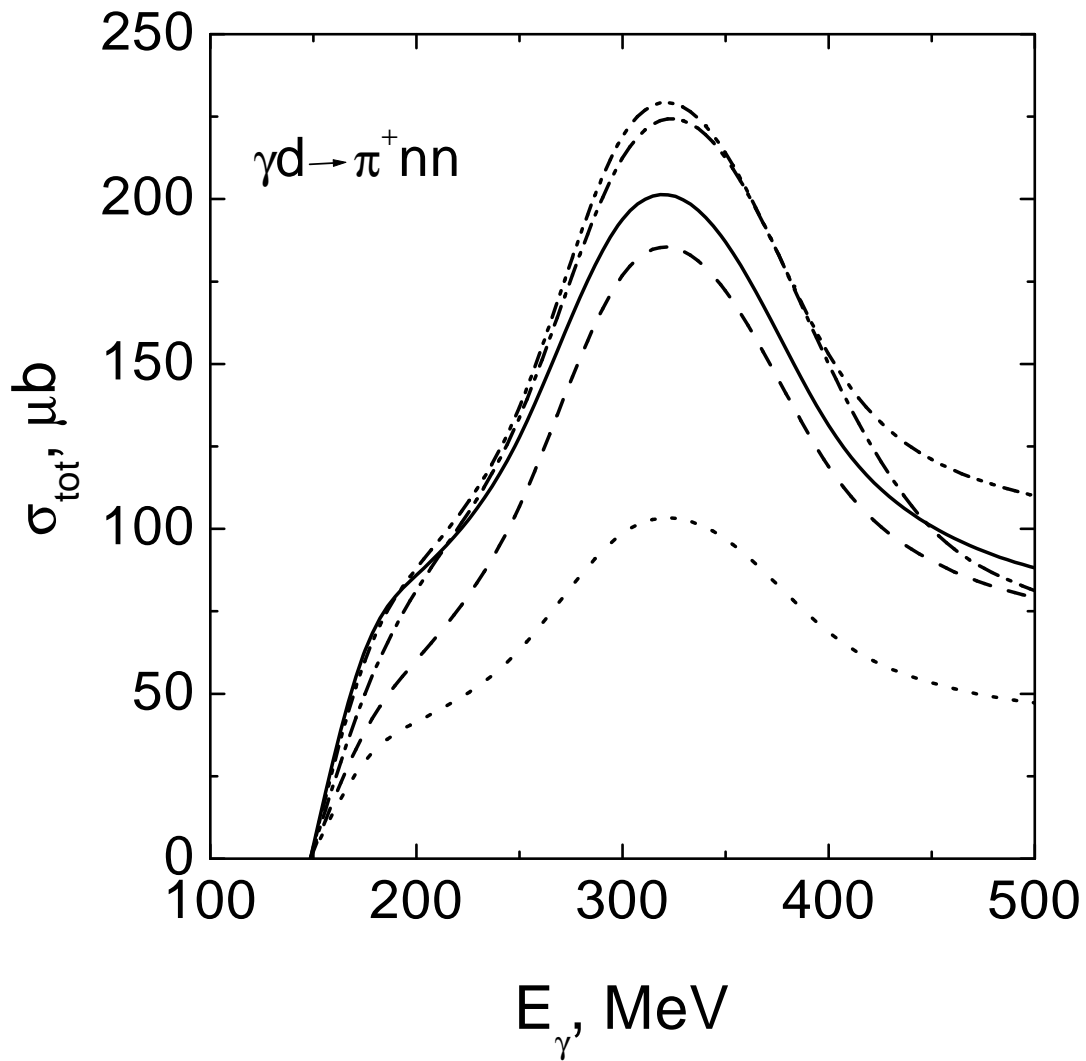


FIG. 7. Total cross section for the reaction  $d(\gamma, \pi^+)nn$ . Meaning of the curves as in Fig. 5.

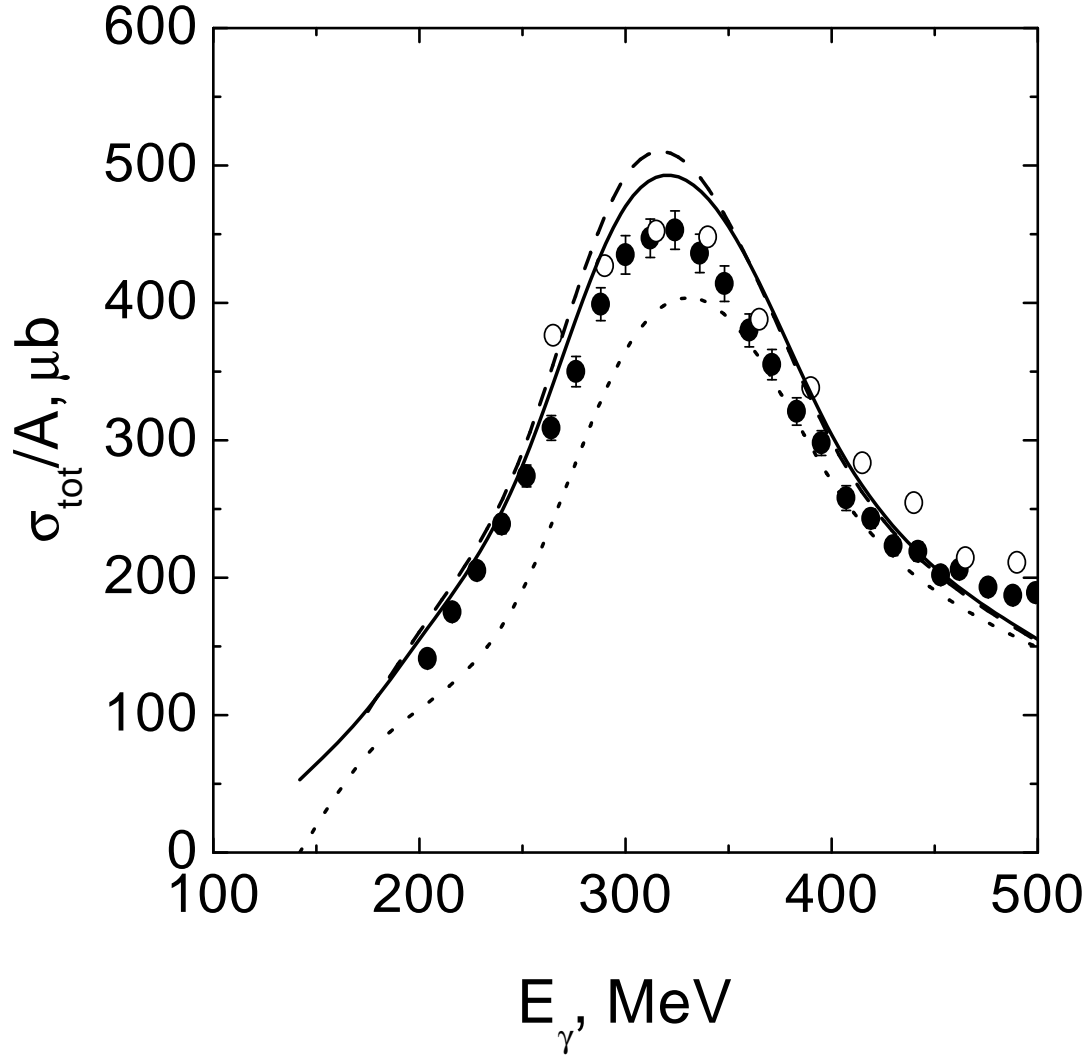


FIG. 8. Total photoabsorption cross section per nucleon for the deuteron from 150 to 500 MeV. Contributions from the reactions  $\gamma d \rightarrow \pi NN$  are shown as dotted curve. Contributions from the reactions  $\gamma d \rightarrow \pi^0 d$  and  $\gamma d \rightarrow np$  are included in the full curve. Results with the MAID multipoles are shown in dashed curve. Data are from Refs. [25] (empty circles) and [26] (solid circles).